

DMD#9902

SELECTIVE METABOLISM OF VINCRISTINE IN VITRO BY CYP3A5

**Jennifer B. Dennison¹, Palaniappan Kulanthaivel¹, Robert J. Barbuch, Jamie L. Renbarger,
William J. Ehlhardt, and Stephen D. Hall**

**Division of Clinical Pharmacology, Department of Medicine, Indiana University School of
Medicine, Indianapolis, IN (JBD,JLR,SDH); Lilly Research Laboratories, A Division of Eli
Lilly and Company, Lilly Corporate Center, Indianapolis, IN (PK,RJB,WDE)**

DMD#9902

Running title: Selective metabolism of vincristine by CYP3A5 in vitro

Corresponding Author: Stephen D. Hall, Ph.D.
Indiana University School of Medicine
Division of Clinical Pharmacology
1001 West 10th St., W7123
Indianapolis, IN 46202

Phone: 317-630-8850

FAX: 317-630-8185

E-mail: sdhall@iupui.edu

Text page: 21

Tables: 4

Figures: 9

References: 35

Abstract: 248 words

Introduction: 535 words

Discussion: 998 words

Abbreviations used are: CYP, Cytochrome P450; Da, Daltons; DQFCOSY, double-quantum filtered correlation spectroscopy; HPLC, high performance liquid chromatography; HMBC, heteronuclear multiple bond correlation; HRP, horse-radish peroxidase; HSQC, heteronuclear single-quantum coherence; LC/MS, liquid chromatography/mass spectrometry; MS/MS, tandem mass spectrometry; NMR, nuclear magnetic resonance spectroscopy; TOCSY, total correlation spectroscopy; VCR, vincristine; VRL, vinorelbine; 1D ZQFTOCSY, one dimensional zero-quantum filtered total correlation spectroscopy.

DMD#9902

Abstract

Clinical outcomes of vincristine therapy, both neurotoxicity and efficacy, are unpredictable, and the reported pharmacokinetics of vincristine have considerable interindividual variability. In vitro and in vivo data support a dominant role for CYP3A enzymes in the elimination of vincristine. Consequently, genetic polymorphisms in CYP expression may contribute to the interindividual variability in clinical response, but the contributions of individual CYPs and the primary pathways of vincristine metabolism have not been defined. In the present study, vincristine was incubated with a library of cDNA-expressed CYPs, and the major oxidative metabolites were identified. CYP3A4 and CYP3A5 were the only CYPs to support substantial loss of parent drug and formation of the previously unidentified, major metabolite (M1). The structure of M1, arising as a result of an oxidative cleavage of the piperidine ring of the dihydrohydroxycantharanthine unit of vincristine, was conclusively established after conversion to suitable derivatives followed by spectroscopic analysis, and a new pathway for vincristine metabolism is proposed. CYP3A5 was more efficient in catalyzing the formation of M1 compared to CYP3A4 (9 to 14-fold higher intrinsic clearance for CYP3A5). The formation of M1 was stimulated (3-fold) by the presence of co-expressed cytochrome *b₅*, but the relative efficiencies of M1 formation by CYP3A4 and CYP3A5 were unaffected. Our findings demonstrate that in contrast to most CYP3A biotransformations, the oxidation of vincristine is considerably more efficient with CYP3A5 than CYP3A4. We conclude that common genetic polymorphisms in CYP3A5 expression may contribute to the interindividual variability in the systemic elimination of vincristine.

Introduction

The treatment of pediatric acute lymphoblastic leukemia (ALL) includes vincristine as one of the core drugs in induction. For these patients, high interindividual variability in efficacy and toxicity with significant differences in outcomes between ethnic groups have been reported. In one acute lymphoblastic leukemia (ALL) study, controlling for compliance, African-American children had a 42% increased mortality rate compared to Caucasian children (Pollock et al., 2000). Event-free-survival (EFS) was only 54% for African-American children compared to a Caucasian EFS of 82% in another ALL study (Lange et al., 2002). Unpredictable but treatment-limiting neurotoxicity has resulted in the arbitrary use of a maximum dose of 2 mg despite known differences in drug exposure between patients (McCune and Lindley, 1997). Early vincristine clinical studies showed up to 11-fold variability in drug exposure (dose-corrected AUC) between adult patients (Van den Berg et al., 1982). More recent pediatric clinical pharmacokinetic studies also reported a 19-fold difference in the dose-corrected AUC (Frost et al., 2003). Understanding determinants of the variation in vincristine exposure may allow identification of patient-specific risk factors for neurotoxicity or individualized dosing strategies to decrease the risk of patient relapse.

Evidence from *in vitro* and *in vivo* studies supports a determinant role for CYP3A-mediated metabolism in the systemic elimination of vincristine. The metabolism of structurally-related compounds, vinblasine and vindesine, with human liver microsomes was inhibited by vincristine and other CYP3A-selective inhibitors which suggest that CYP3A participates in the metabolism of vincristine (Rahmani and Zhou, 1993; Zhou-Pan et al., 1993). In addition, numerous clinical drug-drug interactions with itraconazole and nifedipine have been reported for vincristine, and

DMD#9902

the observed increases in neurotoxicity are consistent with the CYP3A-mediated metabolism of vincristine (Sathiapalan and El-Solh, 2001; Bohme et al., 1995; Kamaluddin et al., 2001; Fedeli et al., 1989). The genetically polymorphic expression of the CYP3A5 enzyme may contribute to the clinically observed interindividual and inter-racial variability in vincristine response. Over 70% of African-Americans have at least one *CYP3A5*1* allele which allows expression of active CYP3A5, but the *CYP3A5*1* allele is only present in 10-20% of Caucasians (Xie et al., 2004). CYP3A4 is normally considered the major metabolizing enzyme in the CYP3A family (Williams et al., 2002). However, for individuals with the *CYP3A5*1* allele, CYP3A5 can represent more than 50% of the total CYP3A content in human liver microsomes (Huang et al., 2004). *CYP3A5* genotype dependent drug clearance is well established for tacrolimus, a substrate oxidized by CYP3A4 and CYP3A5 with relatively equal efficiencies in vitro (MacPhee et al., 2002; Kamdem et al., 2005).

Despite the evidence implicating CYP3A enzymes in the primary metabolic elimination of vincristine, the relative contributions of the drug-metabolizing CYPs to the oxidation of vincristine along with the structural identities of the primary oxidative metabolites remain to be determined (Zhou et al., 1994). These deficiencies preclude an understanding of the genetic and environmental factors that may contribute to the interindividual variability in vincristine disposition. In addition, the roles of primary and subsequent metabolites to the efficacy and toxicity of this important chemotherapeutic agent are unknown. Therefore, the objectives of this study were to identify the major metabolites from the CYP-mediated metabolism of vincristine and to determine the relative contributions of the major drug-metabolizing CYPs to vincristine metabolism in vitro.

DMD#9902

Methods

Chemicals and cDNA-expressed human CYPs

Vincristine sulfate (98%, see Fig. 1 for structure) and peroxidase (Type VI, 298 purpurogallin units/mg) were purchased from Sigma Chemical Co. (St. Louis, MO). [$G-^3H$]vincristine sulfate (3.30 Ci/mmol) was obtained from Amersham Biosciences (Buckinghamshire, UK). NADPH (98%) was purchased from Roche Diagnostics (Indianapolis, IN). cDNA-expressed CYPs co-expressed with CYP-reductase (CYPs 1A1, 1A2, 2A6, 2B6, 2C8, 2C9, 2C19, 2D6, 3A4, 3A5, and 4A11), CYPs co-expressed with CYP-reductase and cytochrome b_5 (CYPs 2J2, 2E1, 3A4, 3A5, and 3A7), and insect cell control microsomes were purchased from the BD Gentest Corporation (“Supersomes,” Woburn, MA). Cytochrome b_5 was purchased from PanVera Corporation (Madison, WI). The manufacturers provided the CYP-reductase activities, protein concentrations, cytochrome b_5 content, and the CYP content as appropriate. All other reagents were of HPLC grade and were purchased from Fisher Scientific (Pittsburgh, PA).

Purification of vincristine

For key experiments, vincristine was purified by HPLC prior to use because vincristine-related impurities were present in the commercially available vincristine, including a compound that co-eluted with the major metabolite M1 (see below). A vincristine standard curve with vinorelbine as an internal standard was used to quantify the concentration of vincristine in the HPLC fractions. Prior to use, the fractions containing purified vincristine were evaporated to dryness at room temperature. 3H -vincristine sulfate was also purified using this procedure.

Incubations with cDNA-expressed CYP enzymes

DMD#9902

All incubations were performed in duplicate. Vincristine (5 μ M) was pre-incubated with CYPs 1A1, 1A2, 2A6, 2B6, 2C8, 2C9, 2C19, 2D6, 2E1, 2J2, 3A4, 3A5, 3A7, and 4A11 (50 pmol of CYP for CYPs 2A6, 2C8, and 2E1; 25 pmol of all CYPs) and insect cell microsomes (control; matched protein content to highest CYP) in a suitable buffer (final volume 250 μ l). Co-expressed cytochrome *b*₅ was present with CYPs 2J2, 2E1, and 3A7. In accord with the recommendation of the manufacturer, CYPs 2A6, 2C9, and 4A11 incubations were performed in 100 mM Tris buffer with 5 mM MgCl₂, pH 7.4 at 37°C and the remainder in 100 mM Na₂HPO₄ buffer with 5 mM MgCl₂, pH 7.4. The reaction was initiated with the addition of NADPH (0.5 mM). After 1 h, the incubation was quenched with an equal volume of acetonitrile, chilled, and centrifuged. The supernatant (50 μ l) was directly assayed by HPLC with UV detection (see below).

To determine the Michaelis-Menten parameters, vincristine (1 to 45 μ M) was pre-incubated with the appropriate CYP and 100 mM Na₂HPO₄ with 5 mM MgCl₂, pH 7.4. The reaction was initiated with the addition of NADPH (0.5 mM). After a set incubation time, the incubation was quenched with an equal volume of acetonitrile, chilled, and centrifuged. The supernatant (25-50 μ l) was directly assayed by HPLC with UV detection. CYP3A activity can be stimulated by the addition or co-expression of cytochrome *b*₅, and this effect may be CYP selective such that activities of CYP3A4 and CYP3A5 may be altered (McCune et al., 2005). Thus, the Michaelis-Menten parameters of CYP3A4 and CYP3A5 were determined with enzyme preparations containing cDNA-expressed enzyme alone, with co-expressed cytochrome *b*₅, and with added cytochrome *b*₅ (PanVera Corp., Madison, WI) at a molar ratio of 3:1 immediately preceding the incubations. To determine any effect of added cytochrome *b*₅, the same lot numbers of CYP3A4

DMD#9902

or CYP3A5 were used with and without cytochrome *b*₅ to minimize variability. The incubation conditions for CYP3A4 (25 or 50 pmol, 15 min, 500 μ l incubation) and CYP3A5 (25 pmol, 3 min, 500 μ l incubation) reactions were determined based on the HPLC assay limits of quantitation and linear conditions. To determine linearity, different CYP concentrations and incubation times were tested, and the best conditions were selected in which less than 15% of the parent was metabolized. Microsomes without CYPs (insect cell control Supersomes) were utilized as negative controls.

For the radiolabelled vincristine incubations, vincristine at approximately 10 μ M (2×10^6 dpm per incubation) was used. CYP3A4 with co-expressed *b*₅ (12.5 pmol), CYP3A5 with co-expressed *b*₅ (25 pmol), and control insect microsomes (matched by CYP3A5 protein content) were incubated with the radiolabelled vincristine for 15 min at a final volume of 250 μ l.

LC/UV/radioactivity analysis

The HPLC system used was an Agilent 1100 Series (Wilmington, DE) and a Hewlett Packard 1050 Series UV detector (Wilmington, DE). Chromatographic separation of M1, M2, vincristine, and vinorelbine (internal standard) was achieved with a C₁₈ column (Inertsil ODS3, 3.0 x 150 mm, 5- μ m particle size; MetaChem Technologies Inc., Torrance, CA) at a flow rate of 0.4 ml/min. The mobile phase consisted of 0.2% formic acid (mobile phase A) and methanol (mobile phase B). Analytes were eluted using a series of linear gradients: 0 min/20% B, 7 min/20% B, 42 min/56% B, 42.1 min/80% B, 52 min/80% B, 52.1 min/20% B. The parent drug and metabolites were detected by ultraviolet absorbance at a wavelength of 254 nm. To allow quantification of M1 by HPLC using a vincristine standard curve, the extinction coefficients of

DMD#9902

M1 and vincristine were determined by synthesizing M1 from radiolabelled vincristine. The extinction coefficients were not statistically different ($p = 0.78$).

The metabolites were also quantified after incubation of radiolabelled vincristine with the CYPs followed by HPLC. Fractions were collected in 20-second aliquots, and the radioactivity of each fraction was determined by liquid scintillation counting (LS3801 scintillation counter; Beckman, Fullerton, CA) with 5 ml of scintillation cocktail (ScintiVerse; Fisher Scientific Co., Fair Lawn, NJ).

Preparation of vincristine metabolites and derivatives

M1 and M1-acetate: Vincristine (not purified) at 30 μ M was pre-incubated with recombinant CYP3A5 (100 pmol) and 100 mM Na₂HPO₄ with 5 mM MgCl₂, pH 7.4 (total volume 1 ml). The reaction was started with the addition of NADPH (0.5 mM final concentration). After 40 min, the incubation was extracted with methylene chloride (1 ml). M1 was then isolated by HPLC (see above), and the appropriate M1 eluent fractions were pooled. The product was extracted with methylene chloride (6 ml), and the solvent was evaporated at room temperature to yield M1. M1-acetate was prepared by mixing M1 and 100 μ l of neat acetic anhydride at room temperature. After 30 min, the reaction was quenched with 200 μ l of water and extracted with methylene chloride (3x1ml). The organic extract was dried and reconstituted in the HPLC mobile phase prior to LC/MS/MS analysis.

M2 with peroxidase: Larger quantities of M2 were prepared by the oxidation of vincristine by horseradish peroxidase (HRP) and hydrogen peroxide, a procedure previously described (Ahn et al., 1997) with slight modifications. Briefly, vincristine sulfate (1.5 mg) was dissolved in 7 ml of

DMD#9902

100 mM Na₂HPO₄ at 37°C. A solution of HRP (1.2 mg), 100 mM Na₂HPO₄ buffer (350 µl), and hydrogen peroxide (125 µl, final reaction concentration 0.4 mM) was added to the vincristine solution and incubated at 37°C in a shaking water bath for 2h. The final mixture was extracted with methylene chloride (6 ml), and the organic extract was dried at room temperature. The residue was purified by HPLC, and the eluent fractions were dried to yield M2 (0.5 mg).

M3: Vincristine (not purified) at 30 µM was pre-incubated with recombinant CYP3A5 (100 pmol) and 100 mM Na₂HPO₄ with 5 mM MgCl₂, pH 7.4 (total volume 1 ml). The reaction was initiated with the addition of NADPH (0.5 mM final concentration). After 40 min, the incubation was quenched with ethyl acetate (0.5 ml) and 5N NaOH (100 µl). Additional ethyl acetate (3 ml) was added, and the organic layer was evaporated. The resulting residue was purified by HPLC as described above to yield M3. M3 was also prepared directly from the purified M1 by mixing M1 with water (1 ml) and 5N NaOH (20 µl) followed by extraction with ethyl acetate (1 ml).

LC/MS analysis

LC/MS analysis was carried out on a Shimadzu VP Series HPLC (Shimadzu Scientific Instruments Inc., Columbia, MD) interfaced with either a triple quadrupole or ion trap mass spectrometer (TSQ Quantum or LTQ mass spectrometer, Thermo Electron Corporation, Waltham, MA). Chromatographic separations were performed on a C₁₈ column (Inertsil ODS-3, 2.1 x 150 mm, 5-µm particle size; MetaChem Technologies, Inc.) with a flow rate of 0.2 ml/min. The mobile phase consisted of 0.2% formic acid (mobile phase A) and methanol (mobile phase B). The analytes were eluted using a series of linear gradients: 0 min/20% B, 3 min/20% B, 28 min/50% B, 45 min/80% B, 50.1 min/20% B. Full scan mass spectra were obtained between 150

DMD#9902

to 1050 Da. Positive ion MS/MS was conducted for the ions of interest using argon as the collision gas at 1.5 mTorr and the collision energy of -40 volts. Accurate mass measurements were performed using a Waters Micromass Q-TOF II quadrupole/orthogonal time-of-flight mass spectrometer (Waters Corporation, Milford, MA). The protonated ion (m/z 311.0814) of sulfadimethoxine (Sigma-Aldrich, St. Louis, MO) was used as the lock mass in all accurate mass determinations.

NMR analysis

NMR spectra were acquired on an Inova 500 MHz NMR system equipped with either a 5 mm cold triple-resonance probe or a 3 mm IFC indirect detection probe (Varian Inc., Palo Alto, CA). Compounds were dissolved in either CD_3OD or $DMSO-d_6$, transferred to a 3 mm NMR tube, and sealed prior to NMR analysis. Proton and carbon chemical shifts were referenced to the residual solvent signals at 3.3 and 49 ppm, respectively, in CD_3OD and at 2.49 and 39.5 ppm, respectively, in $DMSO-d_6$. Two-dimensional NMR experiments including TOCSY, DQFCOSY, HSQC, and HMBC were performed using Varian standard pulse sequences. A selective 1D ZQFTOCSY experiment (Bradley et al., 2005) was performed to identify proton chemical shifts in the extremely crowded regions.

Data Analysis

For incubations with cDNA-expressed CYP3A4 or CYP3A5, the Michaelis-Menten constants (K_m) and maximal rates of metabolism (V_{max}) were determined by fitting the data to a one-enzyme model using non-linear least square regression analysis (WinNonlin 4.0, Pharsight, Mountain View, CA). Statistical significance ($p < 0.05$) was determined using the Student's t

DMD#9902

test or one-way ANOVA for multiple comparisons.

DMD#9902

Results

CYP screen

Screening experiments with a panel of recombinant enzymes revealed that CYP3A4 and CYP3A5 are the major CYPs that metabolize vincristine as shown by parent drug disappearance and M1 formation, the major metabolite (Fig. 2). The vincristine disappearance was normalized to an insect microsomal control, and no M1 was detected in the control. CYPs 3A4, 3A5, 3A7, and 2E1 showed a statistical difference in vincristine disappearance from the control, but only CYP3A4 and CYP3A5 depleted the substrate more than 10%. M1 accounted for 70% and 50% of parent drug loss in the CYP3A5 and CYP3A4 incubations, respectively. M2 accounted for 7% product loss with CYP3A5 and 2% with CYP3A4. M4 formation was also increased over the control for both CYP3A5 and CYP3A4 but only accounted for 1% and 4% of the product loss, respectively.

Vincristine metabolite profiles with CYP3A4 and CYP3A5

Fig. 3 shows the metabolite profile of vincristine with CYP3A5 in which baseline separation was achieved for M1 (21 min), vincristine (VCR, 23 min), and M2 (35 min). M3, a compound formed from M1 under basic conditions, has a retention time of 38 min (peak not shown). Radiolabelled vincristine (10 μ M) was also used to characterize the metabolite formation from 15 min incubations with CYP3A4 and CYP3A5. As shown in Fig. 4, the major metabolite for both CYP3A4 and CYP3A5-mediated metabolism of vincristine was M1. This peak was not present in the insect microsomal control. M2 was present in all samples, but only the CYP3A5 reaction produced levels higher than the control, approximately 10% of M1. Another earlier eluting compound, M4 (19.3-19.7 min), was also present for CYP3A4 and CYP3A5 in larger

DMD#9902

quantities than the control, but the total amount was only 2% of the total radioactivity for both samples. M5 (21.0-21.3 min) was present in the control but was not detectable as a discrete peak in the other incubations because the M1 peak retention time (20.5-20.7 min) was too close to M5 to allow resolution. For the HPLC assay used to determine the kinetic parameters with UV detection, M5 can be distinguished from M1 by retention time. The radioactivity measured from 10 to 45 min represented at least 95% of the radioactivity present in the samples, and no additional peaks with retention times before 10 min or after 45 min were identified.

Structure determination of vincristine metabolites

M2: M2 showed a protonated molecular ion peak at m/z 839, 14 Da higher than that of the corresponding vincristine ion peak. The MS/MS spectrum showed product ions at m/z 471 representing a protonated *N*-formylvindoline (NFV) segment and m/z 369 due to the loss of the NFV segment (a similar ion was observed at m/z 355 for vincristine; Table 1), revealing metabolic changes only in the dihydro-hydroxycatharanthine (DHC) part of the molecule. The molecular weight of M2, 14 Da higher than vincristine, and its molecular formula $C_{46}H_{54}N_4O_{11}$, determined by the accurate mass measurement, led us to believe that M2 could be the same as the previously known metabolite of vincristine obtained by its biotransformation catalyzed either by horseradish peroxidase or ceruloplasmin (Ahn et al., 1997). This hypothesis was further substantiated by a direct comparison of the metabolic products derived from CYP3A5 and horseradish peroxidase reactions of vincristine, which showed identical LC/MS profiles (retention time and MS/MS data) and 1H NMR data. Hence, the structure of M2 is depicted as shown in Fig. 5A. As noted previously by Ahn et al. (1997), the formation of M2 could be rationalized by the oxidation of the carbon α to the piperidine nitrogen followed by the fission of

DMD#9902

C-13 and C-14 bond (Fig. 5A). An analogous oxidative biotransformation pathway has also been reported for leurosine, another dimeric *Vinca* alkaloid, when it was catalyzed by the horseradish peroxidase (Goswami et al., 1988). Furthermore, a similar compound, catharinine, has been reported as a natural product from several *Catharanthus* species (Andriamialisoa RZ et al., 1978) as a result of the C-13 and C-14 bond fission of the piperidine ring probably following the same metabolic reaction from an appropriate precursor in plants.

In the 1997 publication, Ahn et al. have reported only partial NMR chemical shift assignments for M2. Herein, we report the complete (with very few exceptions) proton and carbon chemical shift assignments of M2 in two solvents, namely, CD₃OD and DMSO-*d*₆ (Tables 2 and 3). As noted by Ahn et al. (1997), both with vincristine and M2, we also observed two sets of resonances for M2 in these solvents, but approximately in 4:1 ratio as opposed to 3:2 that was observed by Ahn et al. in CDCl₃. The presence of rotamers in CDCl₃ solutions of 18'-desacetylvincristine was postulated previously as a result of a restricted rotation involving the *N*-formyl group of the NFV moiety (Rao KSPB et al., 1989). In contrast, in the present investigations, we observed this phenomenon only with M2 and not with vincristine and M3 in CD₃OD solutions. In addition, with M2, significant line broadening for most of the resonances was observed in DMSO-*d*₆ at 25°C, however, upon heating to 100°C almost all resonances returned to normal line width with the exception of the formyl proton (H-22'), H-2', and H-8' of the NFV segment, which showed relatively sharper lines at 25°C. The fact that two sets of resonances were still observed when the sample was heated to 120°C may possibly reveal a significantly higher energy barrier between the two rotamers than is normally observed with rotamers due to restricted rotation.

DMD#9902

M1: The initial MS analysis of *M1* either on an ion trap or a triple quadrupole mass spectrometer showed a probable protonated molecular ion peak at m/z 793. However, when analyte was introduced at higher concentrations into the source, an ion at m/z 811 (Fig. 6) was observed corresponding to a molecular formula $C_{45}H_{55}N_4O_{10}$ as determined by accurate mass measurements. Thus, we concluded that the ion at m/z 793 is probably a source induced fragment ion from the protonated molecular ion at m/z 811 due to the loss of water. The MS/MS spectra of the ion at m/z 811 and the source induced ion at m/z 793 showed product ions at m/z 341 and 323, respectively, due to the loss of the NFV component of vincristine suggesting metabolic changes again in the DHC part of the molecule. Attempts to characterize *M1* further by NMR were complicated by the fact that *M1* underwent a spontaneous decomposition during the dry down process following preparatory isolation. As described in the methods section, however, a basic workup of the enzyme reaction mixture produced a stable product *M3*. *M1*, the major component of the CYP3A5-mediated metabolism of vincristine, was observed to a lesser extent in this case suggesting probable formation of *M3* from *M1* upon base treatment. The formation of *M3* from *M1* was additionally confirmed by treating purified *M1* with a base, which yielded *M3* as the dominant product.

The structure of *M3* was unambiguously elucidated by employing a combination of MS and NMR analyses. The molecular formula was determined to be $C_{44}H_{50}N_4O_9$ by accurate mass measurements (protonated molecular ion at m/z 779). This formula represents 32 (CH_4O) and 46 (C_2H_6O) Da less than *M1* and vincristine, respectively. The presence of a product ion at m/z 309 as a result of the loss of NFV from the parent reinforced unaltered NFV segment in *M3* as well.

DMD#9902

Because vincristine and its related analogs are arguably the most complex and highly functionalized members of the indole alkaloid-family, an extensive suite of NMR experiments were required to accurately assign all the proton and carbon chemical shifts and unequivocally establish the structure of its metabolites. The NMR results of M3 reported in Tables 2 and 3 were accomplished after an extensive analysis of ^1H , DQFCOSY, TOCSY, HSQC, HMBC, and 1D ZQFTOCSY spectra. For reliable chemical shift comparisons, vincristine recovered from the CYP3A5 reaction mixture under identical HPLC conditions as that of M3 was used for the NMR experiments to minimize salt induced effects because vincristine is only available commercially as a sulfate salt.

A key, obvious feature observed in the NMR spectrum of M3 when compared to vincristine was the absence of a methoxy resonance ($\text{H}_3\text{-23}$) of the methyl ester in the DHC part of the molecule. Additionally, several deviations in the chemical shifts of key protons (Table 2) and carbons (Table 3) relative to vincristine were also observed. Among them, rather significant departures were observed in the values for both the ethyl side chains. As shown in Table 2, the most dramatic departure was observed for the methylene resonance ($\text{H}_2\text{-20}$) of the DHC ethyl side chain (1.37 ppm in vincristine vs 2.44 ppm in M3) and the methyl resonance ($\text{H}_3\text{-21}'$) of the NFV ethyl side chain (0.79 ppm in vincristine vs 0.07 ppm in M3). The above chemical shift assignments of the ethyl side chains of the respective DHC and NFV segments were established through long-range HMBC correlations observed from the methyl protons at 0.98 ppm ($\text{H}_3\text{-21}$) to a methylene carbon at 36.7 ppm (C-20) and a carbonyl carbon at 212.5 ppm (C-14) and from the other methyl protons at 0.07 ppm ($\text{H}_3\text{-21}'$) to a quaternary carbon at 43.3 ppm (C-16') which in turn showed correlations to the double bond protons at 5.76 (H-14') and 5.14 (H-15') ppm. The

DMD#9902

presence of the unique keto ethyl functionality in the DHC segment of M3 revealed that both M2 and M3 must stem from the same metabolic reaction involving the oxidative cleavage of the piperidine ring.

Initially, the structural relationships between M2 and M1, the putative parent of M3, (28 Da) and M2 and M3 (60 Da) were difficult to reconcile based on the mass differences alone. However, inspection of the diol intermediate, which led to M2 as a result of the cleavage of the C-13 and C-14 bond (Fig. 5A), prompted us to consider an alternative cleavage pathway involving the N-12 and C-13 bond. In fact, such a cleavage should be favored over the C-C bond fission, which led to the formation of M2. As outlined in Fig. 5B, fission of the N-12 and C-13 bond would lead to M1. It is reasonable to assume that the nucleophilic secondary amine thus formed is presumably reactive and under basic conditions underwent an intramolecular amidation reaction leading to the formation of M3 (Fig. 5B). This proposal is consistent with the loss of 32 Da, a mass equivalent of methanol, from M1 during the transition to M3. Furthermore, the absence of a methoxy resonance, as alluded to earlier, in the NMR spectrum of M3 when compared to vincristine is also in accord with this proposal. The formation of the new amide ring and the structure of M3 were fully characterized by the long range HMBC correlations observed from H-11, H-17, and H-18 to a carbonyl carbon at 185.1 ppm (C-22) and other selected correlations as shown in the Fig. 7. Accordingly, in the MS/MS spectrum of M3 distinct product ions were observed at m/z 309, 281, and 237 for the modified DHC moiety (Table 1).

The structure proposed for M1 (precursor of M3) was further supported by the acetylation of M1 immediately following isolation with acetic anhydride, which showed as expected the molecular

DMD#9902

ion peak at m/z 853 and a product ion at m/z 383, 14 Da higher than M2, due to the loss of NFV group. This change in the mass signifies the replacement of the formyl group in M2 by an acetyl group in the acetylated product of M1. The facile loss of water from the protonated molecular ion of M1 (m/z 811) in the mass spectrometer ion source could be explained by the formation of an aminol intermediate as shown in Fig. 8, which then could lose water rapidly in the source to afford the product ion at m/z 793. The reactivity of this newly formed amine could, in part, explain the instability of M1 during the dry down process.

The transformation of vincristine to M3 led to significant structural changes between the two molecules in the DHC unit, and one might anticipate a dramatic conformational departure for M3 from vincristine. The molecular mechanics force field (MMFF) minimized structures of vincristine, and M3 revealed a difference in the disposition of the indole ring of DHC unit with respect to ethyl group of NFV unit. Thus, the pseudo axial distance measured from the methyl of the ethyl group to the indole ring in vincristine is 3.83 Å and in M3 2.16 Å (Kulanthaivel et al., manuscript in preparation). The unusually large diamagnetic shift (Δ -0.72 ppm) observed in the NMR spectrum of M3 for the methyl group (H_3 -21') of the ethyl side chain when compared to vincristine (Table 2) is consistent with the modeling experiments, which suggested a close proximity of the methyl group positioned perpendicular to the indole ring in M3. A similar diamagnetic shift, but to a lesser extent (Δ -0.34 ppm), was observed in M2 for the same methyl group when compared to vincristine suggesting a similar conformational change in M2 due to the fission of the C-13 and C-14 bond.

DMD#9902

M4 and M5: Both M4 and M5 showed identical protonated molecular ion peaks at m/z 823, 2 Da less than the corresponding vincristine ion peak. The structures of M4 and M5 were tentatively proposed as the isomeric epoxides, probably arising as a result of dehydration followed by epoxidation of the resulting C14-C15 double bond of the DHC unit. This is supported by the co-occurrence of vincristine and leurosine in the plant, *Catharanthus roseus*, most likely as a result of similar metabolic changes. The product ion observed at m/z 353 (Table 1) was in concert with the proposed changes in the DHC unit. No additional efforts were taken to further characterize these metabolites.

Enzyme kinetics

The rates of M1 formation were determined for cDNA-expressed CYP3A4 and CYP3A5 (Fig. 9). The K_m and V_{max} values were determined for CYP3A4 and CYP3A5 with and without cytochrome b_5 (Table 4). The presence of cytochrome b_5 consistently increased the V_{max} values for both CYP3A4 and CYP3A5 incubations with the highest V_{max} achieved with co-expressed cytochrome b_5 . The intrinsic clearance values indicated that CYP3A5 selectively metabolized vincristine compared to CYP3A4 for all preparations (9 to 14-fold higher for CYP3A5). The K_m was not statistically different for preparations without b_5 and co-expressed b_5 . The kinetic parameters were not determined for M2 or M4 because the control incubations contained small amounts of these metabolites, and for incubations in the linear range for M1 at the lowest concentrations of vincristine, the amounts of M2 and M4 formed were below the limits of detection. However, the amounts of M2 and M4 were higher than the controls at the highest concentration tested, 48 μ M. Correcting for the amounts in the controls, M2 was less than 10% of the M1 values for both CYP3A5 and CYP3A4 reactions. M4 was approximately 5% of M1

DMD#9902

for CYP3A5 incubations and 15% of M1 for CYP3A4 reactions. The levels of M5 for both CYP3A4 and CYP3A5 reactions were not measurably higher than the controls.

Discussion

Our findings show that vincristine oxidation by CYPs is predominantly mediated by CYP3A4 and CYP3A5. This result is in agreement with clinical reports of drug-drug interactions upon co-administration of vincristine with CYP3A inhibitors such as itraconazole and nifedipine (Sathiapalan and El-Solh, 2001; Bohme et al., 1995; Kamaluddin et al., 2001; Fedeli et al., 1989). The metabolism of vincristine primarily by CYP3A is also consistent with the physico-chemical features of vincristine, in this case, a large molecular volume. In addition, CYP3A4 and CYP3A5 metabolize vincristine to one major metabolite, M1, a novel compound with chemical modifications to the dihydro-hydroxycatharanthine (DHC) part of the molecule, and two minor metabolites, M2 and M4. Previous in vitro experiments with human hepatocytes described the rapid formation of 3 or 4 unknown compounds from the metabolism of vincristine, vinblastine, and vindesine (Zhou et al., 1994). These products may include M1 and the minor metabolites (M2 and M4) that we describe herein or other secondary metabolites. Previously, in vitro studies with structurally related *Vinca* alkaloids, vinblastine and vindesine, showed one major metabolite in human microsomal studies, but the investigators were unable to obtain enough pure material to allow structural identification of the metabolite (Zhou-Pan et al., 1993; Zhou et al., 1993). Beyond scale limitations, the chemical instability of M1 that we observed during standard isolation methods may have hampered previous attempts to identify M1 or its related *Vinca* analogs. We determined the structure of M1 unequivocally by modifying the reactive secondary amine moiety to form two chemically stable derivatives: M3, formed by the base-catalyzed intramolecular amidation of M1, and M1-acetate, generated by acetylation with acetic anhydride. The structures of these compounds as determined by LC/MS/MS and/or NMR analyses in combination with the previously described structure and formation of M2 (Ahn et al., 1997) led

DMD#9902

to the proposal of a new oxidation pathway leading to the formation of M1. In this pathway, M1 shares a common intermediate with M2, formed by the oxidation of C13, α to N-12. While cleavage of the C-13 and C-14 bond resulted in the formation of M2, as documented previously (Ahn et al., 1997), fission of the N-12 and C-13 bond followed by subsequent oxidation and elimination as shown in Fig. 5B resulted in the formation of M1. We believe that the new pathway proposed should be favored over the previously proposed pathway leading to the formation of M2 since chemical cleavage of the C-N bond would be favored over the cleavage of the C-C bond.

In addition to identifying the major metabolite M1, we discovered that CYP3A5 selectively metabolizes vincristine versus CYP3A4, regardless of cytochrome *b*₅ content; for M1 formation CYP3A5 had a 9 to 14-fold higher intrinsic clearance than CYP3A4. For most tested substrates, the CYP3A5 intrinsic clearance is similar or less than that of CYP3A4 (McConn et al., 2004; Huang et al., 2004; Williams et al., 2002; Patki et al., 2003). For example, some studies show a modest selectivity (3-fold) for CYP3A5 with midazolam (Huang et al., 2004), but for other studies, CYP3A5 has equivalent or less activity than CYP3A4 in the formation of 1'-OH-midazolam (Patki et al., 2003; Williams et al., 2002; Walsky and Obach, 2004). Recently, another study on the metabolism of buprenorphine showed the selective metabolism by CYP3A5 versus CYP3A4 in a screening experiment, but rigorous enzyme kinetics were not presented (Chang et al., 2005). Thus, our findings with vincristine, which show an order of magnitude greater intrinsic clearance values, provide an unusual example of a very high selectivity for CYP3A5.

DMD#9902

The selective metabolism of vincristine by CYP3A5 may be clinically important because CYP3A5 is polymorphically expressed. CYP3A5 is expressed in approximately 70% of African-Americans have at least one *CYP3A5*1* allele which allows expression of significant quantities of active CYP3A5, but the *CYP3A5*1* allele is only present in 10-20% of Caucasians (Xie et al., 2004). The most common allelic variants include *CYP3A5*3*, *CYP3A5*6*, and *CYP3A5*7*. For the *CYP3A5*3* genotype, a single nucleotide polymorphism (SNP) in intron 3 creates a consensus splice site that after processing leads to a premature termination codon (Kuehl et al., 2001). The less common *CYP3A5*6* and *CYP3A5*7* allelic variants also result in the expression of little to no active CYP3A5 (Kuehl et al., 2001). Because such a small amount of active CYP3A5 is produced in individuals without the *CYP3A5*1* allele, the other genotypes described are effectively void of active CYP3A5.

Polymorphic CYP3A5 expression may in part explain interracial differences in vincristine efficacy (Pollock et al., 2000; Lange et al., 2002). Clinical studies that evaluated the impact of *CYP3A5* genotype on drug disposition have been confounded by the variability in CYP3A4 expression and often show substrate dependence. Studies with midazolam, a common CYP3A probe, have shown mixed results. Some clinical studies showed increased metabolism for *CYP3A5*1* carriers (Wong et al., 2004; Yu et al., 2004), but other studies did not find a statistical difference between the groups (Floyd et al., 2003; Shih and Huang, 2002). For other CYP3A substrates, such as tacrolimus, drug disposition is dependent upon *CYP3A5* genotype. For example, in an organ transplant study, patients with *CYP3A5*3/*3* required less drug to reach the required therapeutic trough concentrations compared with *CYP3A5*1* carriers (Hesselink et al., 2003). This result is consistent with the clinical evidence that African-Americans have a poorer

DMD#9902

outcome following solid organ transplantation (Nair et al., 2002). Interestingly, in vitro studies showed that the intrinsic clearances of tacrolimus with recombinant CYP3A4 and CYP3A5 were similar with less than a 2-fold selectivity by CYP3A5 (Kamdem et al., 2005) compared to the 9 to 14-fold selectivity we report for vincristine. Therefore, if the in vitro model is representative of human metabolism, the CYP3A5 contribution to vincristine metabolism may be even more clinically relevant than tacrolimus. Based on our results of selective metabolism by CYP3A5, it seems particularly important to evaluate the impact of *CYP3A5* genotype on the pharmacokinetics of vincristine. This type of study may allow more individualized dosing strategies, which could improve clinical outcomes in cancers that include vincristine in their treatment.

DMD#9902

Acknowledgements

We thank Jeffery J. Alberts for the accurate mass measurements and David R. Jones for his technical assistance.

DMD#9902

References

- Ahn SH, Duffel MW and Rosazza JP (1997) Oxidations of vincristine catalyzed by peroxidase and ceruloplasmin. *J Nat Prod* **60**:1125-1129.
- Andriamialisoa RZ, Langlois N, Potier P, Chiaroni a and Riche C (1978) The structure of catharanthine: bisindolic "alkaloid" isolated from several *Catharanthus* species. *Tetrahedron* **34**:677-683.
- Bohme A, Ganser A and Hoelzer D (1995) Aggravation of vincristine-induced neurotoxicity by itraconazole in the treatment of adult ALL. *Annals of Hematology* **71**:311-312.
- Bradley SA, Krishnamurthy K and Hu H (2005) Simplifying DOSY spectra with selective TOCSY edited preparation. *J Magn Reson* **172**:110-117.
- Chang Y, Moody DE and Cance-Katz EF (2005) Novel metabolites of buprenorphine detected in human liver microsomes and human urine. *Drug Metab Dispos.* **34**: 440-448.
- Fedeli L, Colozza M, Boschetti E, Sabalich I, Aristei C, Guerciolini R, Del Favero A, Rossetti R, Tonato M, Rambotti P and Davis S (1989) Pharmacokinetics of vincristine in cancer patients treated with nifedipine. *Cancer* **64**:1805-1811.
- Floyd MD, Gervasini G, Masica AL, Mayo G, George AL, Jr., Bhat K, Kim RB and Wilkinson GR (2003) Genotype-phenotype associations for common CYP3A4 and CYP3A5 variants in the basal and induced metabolism of midazolam in European- and African-American men and women. *Pharmacogenetics* **13**:595-606.
- Frost BM, Lonnerholm G, Koopmans P, Abrahamsson J, Behrendtz M, Castor A, Forestier E, Uges DR and de Graaf SS (2003) Vincristine in childhood leukaemia: no pharmacokinetic rationale for dose reduction in adolescents. *Acta Paediatr* **92**:551-557.

DMD#9902

- Goswami A, Macdonald TL, Hubbard C, Duffel MW and Rosazza JP (1988) Leurosine biotransformations: an unusual ring-fission reaction catalyzed by peroxidase. *Chem Res Toxicol* **1**:238-242.
- Hesselink DA, van Schaik RH, van dH, I, van der WM, Gregoor PJ, Lindemans J, Weimar W and van GT (2003) Genetic polymorphisms of the CYP3A4, CYP3A5, and MDR-1 genes and pharmacokinetics of the calcineurin inhibitors cyclosporine and tacrolimus. *Clin Pharmacol Ther* **74**:245-254.
- Huang W, Lin YS, McConn DJ, Calamia JC, Totah RA, Isoherranen N, Glodowski M and Thummel KE (2004) Evidence of significant contribution from CYP3A5 to hepatic drug metabolism. *Drug Metab Dispos* **32**:1434-1445.
- Kamaluddin M, McNally P, Breatnach F, O'Marcaigh A, Webb D, O'Dell E, Scanlon P, Butler K and O'Meara A (2001) Potentiation of vincristine toxicity by itraconazole in children with lymphoid malignancies. *Acta Paediatrica* **90**:1204-1207.
- Kamdern LK, Streit F, Zanger UM, Brockmoller J, Oellerich M, Armstrong VW and Wojnowski L (2005) Contribution of CYP3A5 to the in vitro hepatic clearance of tacrolimus. *Clin Chem* **51**:1374-1381.
- Kuehl P, Zhang J, Lin Y, Lamba J, Assem M, Schuetz J, Watkins P, Daly A, Wrighton S, Hall S, Maurel P, Relling M, Brimer C, Yasuda K, Venkataramanan R, Strom S, Thummel K, Boguski M and Schuetz E (2001) Sequence diversity in CYP3A promoters and characterization of the genetic basis of polymorphic CYP3A5 expression. *Nature Genetics* **27**:383-391.
- Lange BJ, Bostrom BC, Cherlow JM, Sensel MG, La MK, Rackoff W, Heerema NA, Wimmer RS, Trigg ME and Sather HN (2002) Double-delayed intensification improves event-free

DMD#9902

survival for children with intermediate-risk acute lymphoblastic leukemia: a report from the Children's Cancer Group. *Blood* **99**:825-833.

MacPhee IA, Fredericks S, Tai T, Syrris P, Carter ND, Johnston A, Goldberg L and Holt DW (2002) Tacrolimus pharmacogenetics: polymorphisms associated with expression of cytochrome p4503A5 and P-glycoprotein correlate with dose requirement. *Transplantation* **74**:1486-1489.

McConn DJ, Lin YS, Allen K, Kunze KL and Thummel KE (2004) Differences in the inhibition of cytochromes P450 3A4 and 3A5 by metabolite-inhibitor complex-forming drugs. *Drug Metab Dispos* **32**:1083-1091.

McCune J and Lindley C (1997) Appropriateness of maximum dose guidelines for vincristine. *American Journal of Health Systems Pharmacy* **54**:1755-1758.

McCune JS, Risler LJ, Phillips BR, Thummel KE, Blough D and Shen DD (2005) Contribution of CYP3A5 to hepatic and renal ifosfamide N-dechloroethylation. *Drug Metab Dispos* **33**:1074-1081.

Nair S, Eustace J and Thuluvath P (2002) Effect of race on outcome of orthotopic liver transplantation: a cohort study. *Lancet* **359**:287-293.

Patki KC, Von Moltke LL and Greenblatt DJ (2003) In vitro metabolism of midazolam, triazolam, nifedipine, and testosterone by human liver microsomes and recombinant cytochromes p450: role of cyp3a4 and cyp3a5. *Drug Metab Dispos* **31**:938-944.

Pollock B, DeBaun M, Camitta B, Shuster J, Ravindranath Y, Pullen D, Land V, Mahoney DJ, Lauer S and Murphy S (2000) Racial differences in the survival of childhood B-precursor acute lymphoblastic leukemia: a Pediatric Oncology Group Study. *Journal of Clinical Oncology* **18**:813-823.

DMD#9902

- Rahmani R and Zhou X (1993) Pharmacokinetics and metabolism of vinca alkaloids. *Cancer Surveys* **17**:269-281.
- Rao KSPB, De Bruyn A, Trouet A, Verzele M and Hannart J (1989) Proton NMR and carbon-13 NMR study of two vincristine derivatives at 300 MHz. *J Bull Soc Chim Belg* **98**:125-132.
- Sathiapalan RK and El-Solh H (2001) Enhanced vincristine neurotoxicity from drug interactions: case report and review of literature. *Pediatr Hematol Oncol* **18**:543-546.
- Shih PS and Huang JD (2002) Pharmacokinetics of midazolam and 1'-hydroxymidazolam in Chinese with different CYP3A5 genotypes. *Drug Metab Dispos* **30**:1491-1496.
- Van den Berg H, Desai Z, Wilson R, Kennedy G, Bridges J and Shanks R (1982) The pharmacokinetics of vincristine in man: reduced drug clearance associated with raised serum alkaline phosphatase and dose-limited elimination. *Cancer Chemotherapy and Pharmacology* **8**:215-219.
- Walsky RL and Obach RS (2004) Validated assays for human cytochrome P450 activities. *Drug Metab Dispos* **32**:647-660.
- Williams JA, Ring BJ, Cantrell VE, Jones DR, Eckstein J, Ruterbories K, Hamman MA, Hall SD and Wrighton SA (2002) Comparative metabolic capabilities of CYP3A4, CYP3A5, and CYP3A7. *Drug Metab Dispos* **30**:883-891.
- Wong M, Balleine RL, Collins M, Liddle C, Clarke CL and Gurney H (2004) CYP3A5 genotype and midazolam clearance in Australian patients receiving chemotherapy. *Clin Pharmacol Ther* **75**:529-538.
- Xie HG, Wood AJ, Kim RB, Stein CM and Wilkinson GR (2004) Genetic variability in CYP3A5 and its possible consequences. *Pharmacogenomics* **5**:243-272.

DMD#9902

Yu KS, Cho JY, Jang IJ, Hong KS, Chung JY, Kim JR, Lim HS, Oh DS, Yi SY, Liu KH, Shin JG and Shin SG (2004) Effect of the CYP3A5 genotype on the pharmacokinetics of intravenous midazolam during inhibited and induced metabolic states. *Clin Pharmacol Ther* **76**:104-112.

Zhou X, Placidi M and Rahmani R (1994) Uptake and metabolism of vinca alkaloids by freshly isolated human hepatocytes in suspension. *Anticancer Research* **14**:1017-1022.

Zhou X, Zhou-Pan X, Gauthier T, Placidi M, Maurel P and Rahmani R (1993) Human liver microsomal cytochrome P450 3A isozymes mediated vindesine biotransformation. *Biochemical Pharmacology* **45**:853-861.

Zhou-Pan X, Seree E, Zhou X, Placidi M, Maurel P, Barra Y and Rahmani R (1993) Involvement of human liver cytochrome P450 3A in vinblastine metabolism: drug interactions. *Cancer Research* **53**:5121-5126.

DMD#9902

Footnotes

This study was funded by the National Institute of Health (1 K23 RR019956-01).

¹ Authors are equal contributors to this publication.

Legend for Figures

Fig. 1. Structure of vincristine.

Fig. 2. Vincristine disappearance and M1 formation for various CYPs. All enzymes were tested in duplicate (25 or 50 pmol, 5 μ M vincristine, 250 μ l final volume). Vincristine and M1 concentrations were compared to an internal standard and normalized to the average of an insect microsomal control. The enzymes were tested in the absence of cytochrome *b*₅ with the exception of coexpressed *b*₅ in CYPs 2J2, 2E1, and 3A7. Error bars represent data ranges (N=2) for each CYP. Statistical differences from the control incubations were calculated for vincristine disappearance using one-way ANOVA analysis, **p*<0.05, ***p*<0.01, ****p*<0.001.

Fig. 3. Representative HPLC chromatogram of CYP3A5-mediated metabolism of vincristine (VCR) (50 pmol CYP3A5, 20 μ M vincristine, 500 μ l final volume). The retention times of M1, the major metabolite, and M2, a minor metabolite, are identified. Vinorelbine (VRL) is used as an internal standard.

Fig. 4. Radiochromatograms of 10 μ M ³H-vincristine incubations for 15 min with (A) insect control microsomes, matched to CYP3A5 protein content, (B) cDNA-expressed CYP3A4 with co-expressed *b*₅, 50 pmol/ml (C) and CYP3A5 with co-expressed *b*₅, 100 pmol/ml. At least 95% of the radioactivity is represented from 10 to 45 min, and no distinctive peaks different than the control are present outside of this time range. All dpm values are normalized to total radioactivity recovered.

Fig. 5. Proposed biotransformation pathways of vincristine catalyzed by CYP3A4 and CYP3A5. A, formation of M2; B, formation of M1 and M3.

Fig. 6. Full scan mass spectrum of M1. The ions at *m/z* 406 and 397 are the doubly charged molecular ion and the source induced dehydration ion, respectively.

DMD#9902

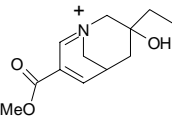
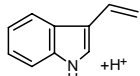
Fig. 7. Selected ^1H - ^{13}C HMBC correlations of M3. The J -filter was optimized for $^1J_{\text{C-H}} = 140$ Hz and N bond delay was set to 0.063 sec corresponding to $^{\text{N}}J_{\text{C-H}} = 8$ Hz.

Fig. 8. Mechanism of formation of M1 fragment ion at m/z 793 in MS ion source.

Fig. 9. Rate of M1 formation normalized to incubation time during CYP3A4 and CYP3A5-mediated metabolism of vincristine with co-expressed cytochrome b_5 (●), exogenous b_5 (3:1) (▼), and no b_5 (○). Data was fit to a one-enzyme model to determine Michaelis-Menten parameters. Replicate data was not available for M1 formation with CYP3A5 and exogenous b_5 .

DMD#9902

Table 1: Proposed product ion assignments for vincristine (VCR) and its metabolites

Product Ion Assignment	VCR	M1	M1 Acetate	M2	M3	M4 ^a
M+H ⁺	825	811 ^b	853	839	779	823
- H ₂ O	807	793 ^c	835	821	761	805
- O=C=CH ₂	783	769	811	797	737	781
- AcOH or MeOFm	765	751	793	779	719	763
- AcOH or MeOFm - H ₂ O	747	733 ^c	775	761	701	745
- AcOH or MeOFm - O=C=CH ₂	723	709	751	737	677	721
- AcOH or MeOFm - AcOH or MeOFm	705	691	733	719	659	703
- AcOH or MeOFm - AcOH or MeOFm - H ₂ O	687	673 ^c	N.D.	701	641	685
- Neutral [A]	599	585	627	613	N.D.	N.D.
- Neutral [A] - CO	N.A.	N.A.	599	585	N.A.	N.A.
- Neutral [A] - O=C=CH ₂	N.A.	N.A.	585	N.A.	N.A.	N.A.
NFV + H ion	N.D.	N.D.	471	471	N.D.	N.D.
NFV ion	N.D.	469	469	N.D.	469	N.D.
NFV + H ion - AcOH or MeOFm	N.D.	N.D.	411	411	N.D.	N.D.
NFV ion - AcOH or MeOFm	N.D.	N.D.	409	N.D.	409	N.D.
- NFV	355	341	383	369	309	353
m/z 355 - H ₂	353	N.A.	N.A.	N.A.	N.A.	N.A.
- NFV - H ₂ O	N.A.	323 ^c	N.A.	351	N.A.	N.A.
- NFV - MeOH	N.D.	309	351	337	N.A.	321
- NFV - AcOH or MeOFm	N.D.	281	323	309	N.D.	293
- NFV - 2-butanone	N.A.	N.D.	N.D.	N.D.	N.D.	281
m/z 309 - 2-butanone	N.A.	237	N.A.	237	237	N.A.
- NFV - CO for M2 and M3 and O=C=CH ₂ for M1 acetate	N.A.	N.A.	341	341	281	N.A.
	224 ^d	N.A.	N.A.	N.A.	N.A.	N.D.
	144	144 ^c	N.D.	144	144	N.D.

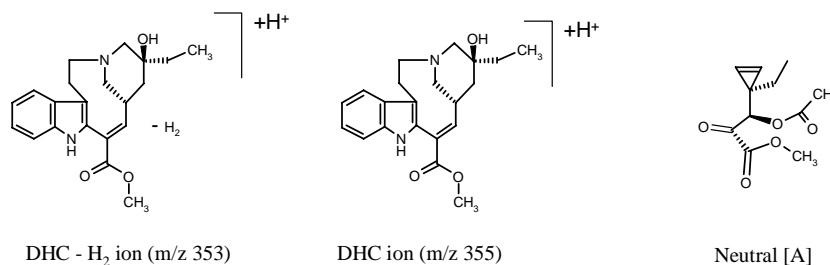
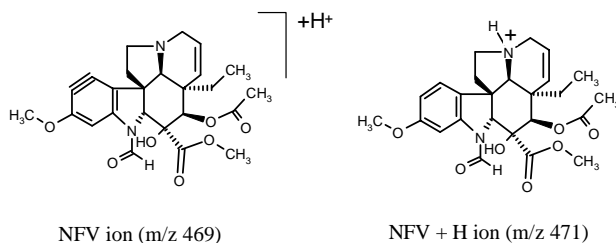
^aIdentical product ions were observed for M5. M4 and M5 showed additional ions at m/z 694 (loss of C₉H₇N), 680 (loss of C₁₀H₉N), 634 (loss of MeOFm or AcOH from m/z 694), and 620 (loss of MeOFm or AcOH from m/z 680).

^bThis ion was not always observed.

^cThe ion at m/z 793 was observed as a source induced fragment ion in the full scan spectrum. The additional ions as indicated were only observed as product ions from m/z 793.

^dThe elemental composition of this ion was confirmed with accurate mass determinations.

AcOH, acetic acid; MeOFm, methyl formate; NFV, *N*-formylvindoline; N.A., not applicable; N.D., not determined.



DMD#9902

Table 2: Proton chemical shift assignments of vincristine, M2, and M3

Position	δ_H multiplicity (<i>J</i> in Hz)			
	Vincristine ^{a,b}	M2 ^b	M2 ^c	M3 ^b
5	7.46 d (8)	7.52 d (8)	7.50 d (8)	7.51 d (8)
6	7.02 t (8)	7.01 t (8)	6.97 t (8)	7.04 t (8)
7	7.09 t (8)	7.06 t (8)	7.03 t (8)	7.15 t (8)
8	7.26 d (8)	7.19 overlapped	7.30 d (8)	7.39 d (8)
10a	4.18 dd (15.5, 10)	3.47 overlapped	3.29 overlapped	3.10 overlapped
10b	3.15 dd (15.5, 5.5)	3.16 overlapped	3.06 overlapped	3.01 dd (15, 6)
11a	3.36 obsc	3.62 overlapped	3.48 overlapped	4.14 dd (12.5, 7)
11b		3.51 overlapped		2.94 dt (6, 12)
13a	2.92 d (14.5)	7.35 br s	7.41 s	-
13b	2.86 d (14.5)	-	-	-
14	-	-	-	-
15a	1.55 overlapped	2.12 overlapped	2.03 AB ^d	2.67 overlapped
15b	1.45 overlapped			
16	0.87 m	2.33 m	2.11 m ^d	2.13 m
17a	3.51 d (14)	3.51 overlapped	3.23 dd (14,2.5) ^d	3.11 dd (12.5, 6.5) ^d
17b	2.52 dd (14, 4.5)	3.04 m	2.95 overlapped ^d	3.05 dd (12.5, 3.3) ^d
18a	4.06 dd (15.5, 14)	3.14 overlapped	2.97 dd (16, 6.5) ^d	2.76 dd (13.5, 6)
18b	2.37 dd (15.5, 4)	2.21 overlapped	2.20 br d (16.5) ^d	2.67 overlapped
19	-	-	-	-
20a	1.37 q (7.5)	2.17 overlapped	2.10 m	2.44 q (7.5)
20b		1.77 m	1.81 m	
21	0.91 t (7.5)	0.80 t (7)	0.74 t (7.5)	0.98 t (7.5)
23	3.69 s	3.59 s	3.52 br s	-
2'	4.58 s	4.64 s	4.52 s	4.60 s
5'	6.90 s	6.97 br s	6.90 s	6.72 s
8'	7.23 s	7.20 s	7.30 very br	7.17 s
10a'	2.09 ddd (13, 9, 4)	2.30 overlapped	2.23 overlapped	2.20 obsc
10b'	1.78 dt (6.5, 12.5)	2.06 overlapped	2.04 overlapped	2.10 overlapped
11a'	3.28 obsc	3.36 overlapped	3.28 overlapped	3.36 dt (7, 10.5) ^d
11b'	2.61 dt (3.5, 11)	2.74 dt (11, 3.5)	2.54 overlapped	2.57 dt (4.5, 11)
13a'	3.29 obsc	3.36 overlapped	3.31 overlapped	3.28 obsc
13b'	2.85 br d (15.5)	2.91 br d (16)	2.74 br d (16)	2.72 br d (16)
14'	5.89 dd (10, 5)	5.90 dd (10, 5)	5.83 dd (10, 4.8)	5.76 dd (10, 4.8)
15'	5.41 d (10)	5.41 d (10)	5.32 d (10)	5.14 d (10)
17'	3.03 s	3.10 s	2.86 s	2.63 s
18'	5.15 s	5.14 s	5.01 s	4.95 s
20a'	1.54 overlapped	1.44 m	1.40 m	1.20 dq (15, 7.5)
20b'	1.41 overlapped		1.30 m	0.78 dq (15, 7.5)
21'	0.79 t (7.5)	0.45 br t (6)	0.47 t (7)	0.07 t (7.5)
22'	8.93 s	9.01 s	^e	8.86 s
23'	3.91 s	3.85 s	3.76 s	3.95 s
25'	2.00 s	2.02 s	1.93 s	1.91 s
27'	3.63 s	3.63 s	3.56 s	3.60 s

^aVincristine used was isolated from the CYP3A5 incubation mixture.

^bIn CD₃OD at 25°C.

^cIn DMSO-*d*₆ at 100°C.

^dAssignments either made or confirmed by selective 1D ZQFTOCSY experiment.

^eVery broad peak with peak width >1 ppm. This peak was observed at 9.04 ppm (br s) at 25°C

s, singlet; d, doublet; t, triplet; q, quartet; dd, double doublet; dt, double triplet; AB, center of AB spin system; m, multiplet; br, broad.

DMD#9902

Table 3: Carbon chemical shift assignments of vincristine, M2, and M3.

Position	δ_c			
	Vincristine ^{a,b}	M2 ^b	M2 ^{c,d}	M3 ^b
2	130.5	N.D.	N.D.	134.1
3	117.5	119.0	N.D.	111.6
4	129.9	129.0	N.D.	128.8
5	118.6	118.2	116.9	118.8
6	119.8	119.8	118.0	119.7
7	123.1	122.9	120.8	122.7
8	112.2	112.3	110.9	111.4
9	136.9	137.2	N.D.	136.6
10	26.1	25.6	24.5	20.6
11	57.4	50.7	48.2	55.7
13	63.3	165.5	162.5	-
14	69.1	211.9	N.D.	212.5
15	39.8	50.1	47.9	46.2
16	29.6	30.4	29.0	27.9
17	47.0	52.6	N.D.	57.1
18	35.7	38.7	36.7	41.2
19	57.0	N.D.	N.D.	57.7
20	35.5	35.8	33.8	36.7
21	6.9	7.8	6.8	7.7
22	176.2	175.5	N.D.	185.1
23	52.6	52.5	50.9	-
2'	72.8	72.7	71.8	72.8
3'	54.0	54.0	N.D.	53.7
4'	125.2	124.9	N.D.	124.7
5'	125.9	128.2	125.2	125.5
6'	129.1	127.8	N.D.	129.4
7'	159.4	159.1	N.D.	159.5
8'	96.6	96.1	N.D.	96.9
9'	142.5	142.5	N.D.	141.6
10'	42.3	41.3	39.9	41.0
11'	49.3	49.5	48.4	50.1
13'	50.7	50.6	49.1	50.7
14'	125.7	125.8	123.6	125.4
15'	130.8	130.9	129.4	130.8
16'	43.7	43.3	N.D.	43.3
17'	64.8	64.0	63.2	65.1
18'	77.9	78.4	76.1	77.8
19'	80.7	80.9	N.D.	80.5
20'	31.7	31.3	29.8	31.1
21'	8.4	7.5	6.4	6.5
22'	162.8	162.4	N.D.	162.8
23'	56.6	56.4	55.5	56.1
24'	171.6	171.9	N.D.	171.0
25'	20.5	20.5	19.9	20.4
26'	171.8	171.6	N.D.	171.7
27'	52.8	52.8	51.5	52.9

^aVincristine used was isolated from the CYP3A5 incubation mixture.

^bIn CD₃OD at 25°C.

^cIn DMSO-*d*₆ at 100°C.

^dOnly carbons bearing protons were assigned.

N.D., not detected.

DMD#9902

Table 4. Michaelis-Menten parameters for M1 formation with CYP3A4 and CYP3A5

V_{max} units = pmol M1/pmol CYP/min, K_m units = μ M, fitted values \pm 1 standard deviation, $Cl_{int} = V_{max}/K_m$

	No b_5			Exogenous b_5 (3:1 ratio)			Co-expressed b_5		
	CYP3A4	CYP3A5	<i>p</i> -value	CYP3A4	CYP3A5	<i>p</i> -value	CYP3A4	CYP3A5	<i>p</i> -value
V_{max}	0.90 \pm 0.06	8.1 \pm 0.4	<0.0001	1.49 \pm 0.07	11.0 \pm 1.0	<0.0001	2.97 \pm 0.17	21.5 \pm 0.9	<0.0001
K_m	19.7 \pm 3.0	14.3 \pm 1.7	0.14	25.7 \pm 2.6	13.3 \pm 3.2	0.009	19.9 \pm 2.5	16.7 \pm 1.6	0.30
Cl_{int}	0.046 \pm 0.004	0.57 \pm 0.04	<0.0001	0.058 \pm 0.003	0.83 \pm 0.13	<0.0001	0.15 \pm 0.01	1.29 \pm 0.08	<0.0001

Fig. 1

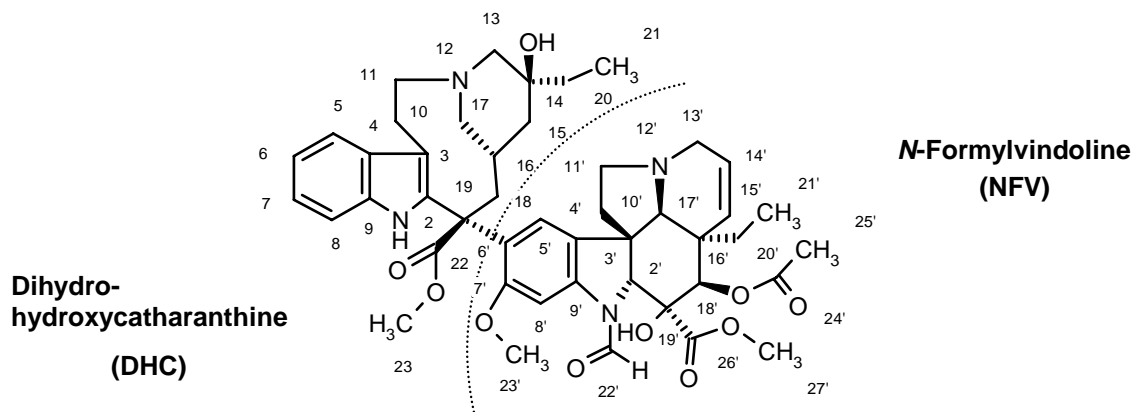


Fig. 2

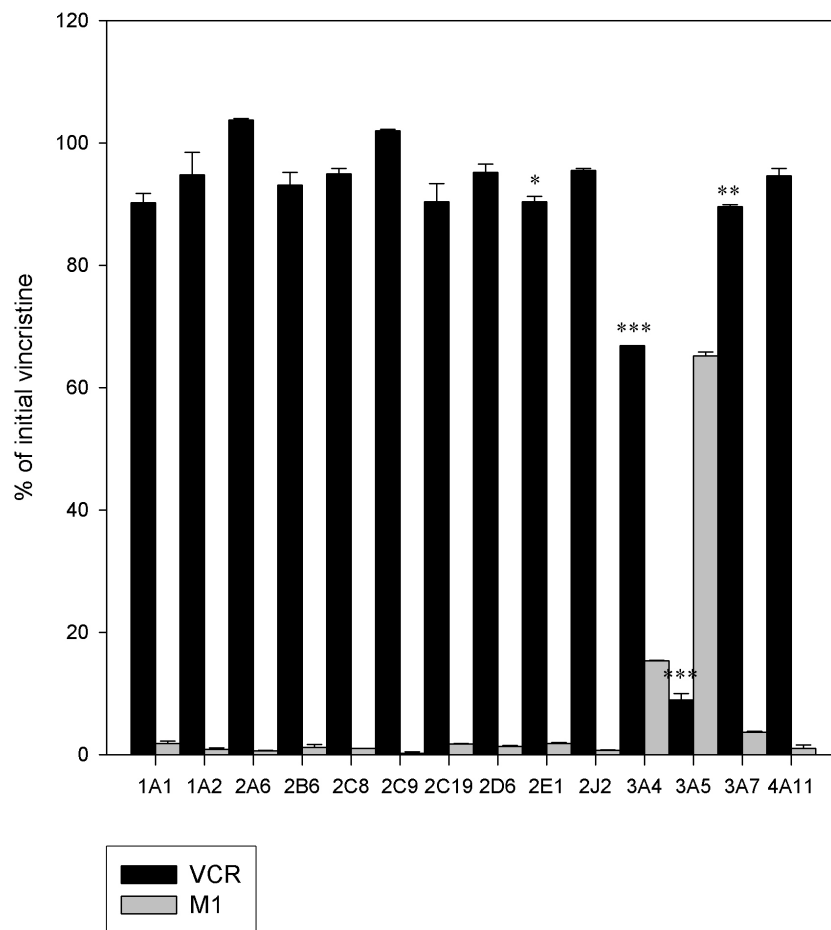


Fig. 3

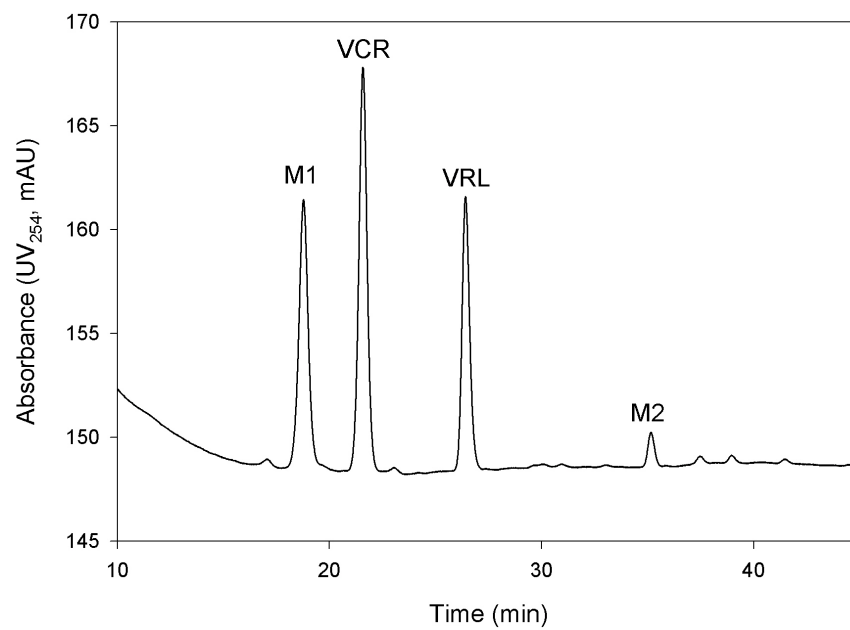


Fig. 4

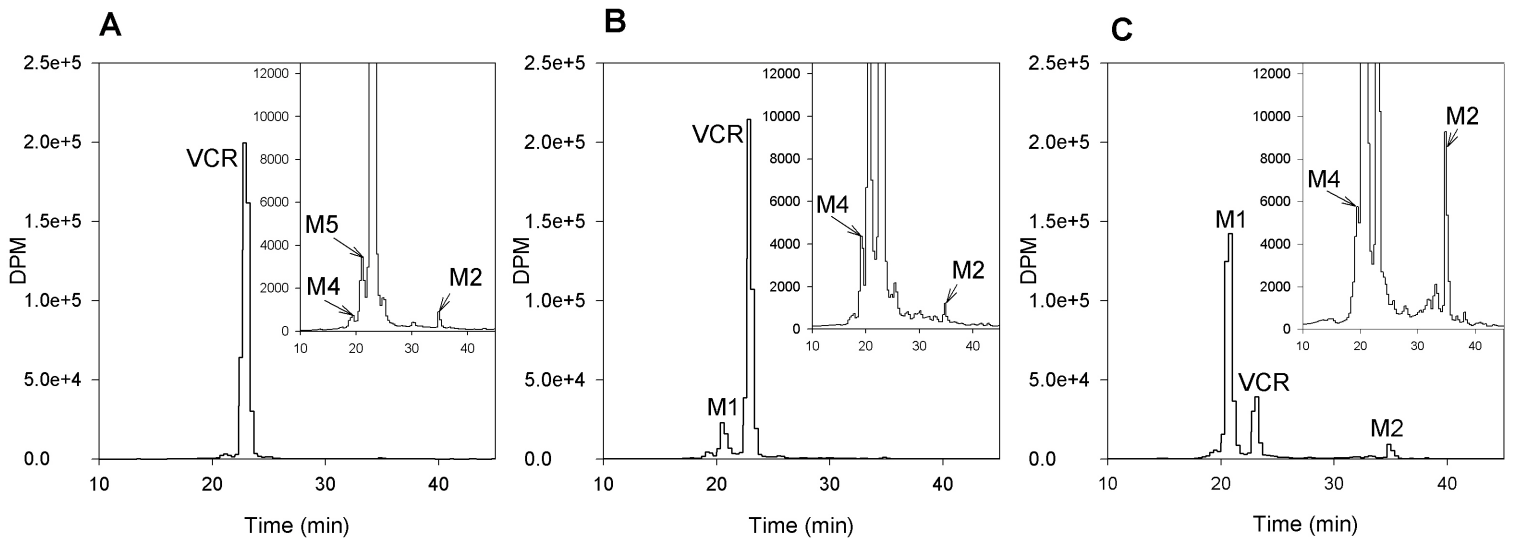


Fig. 5

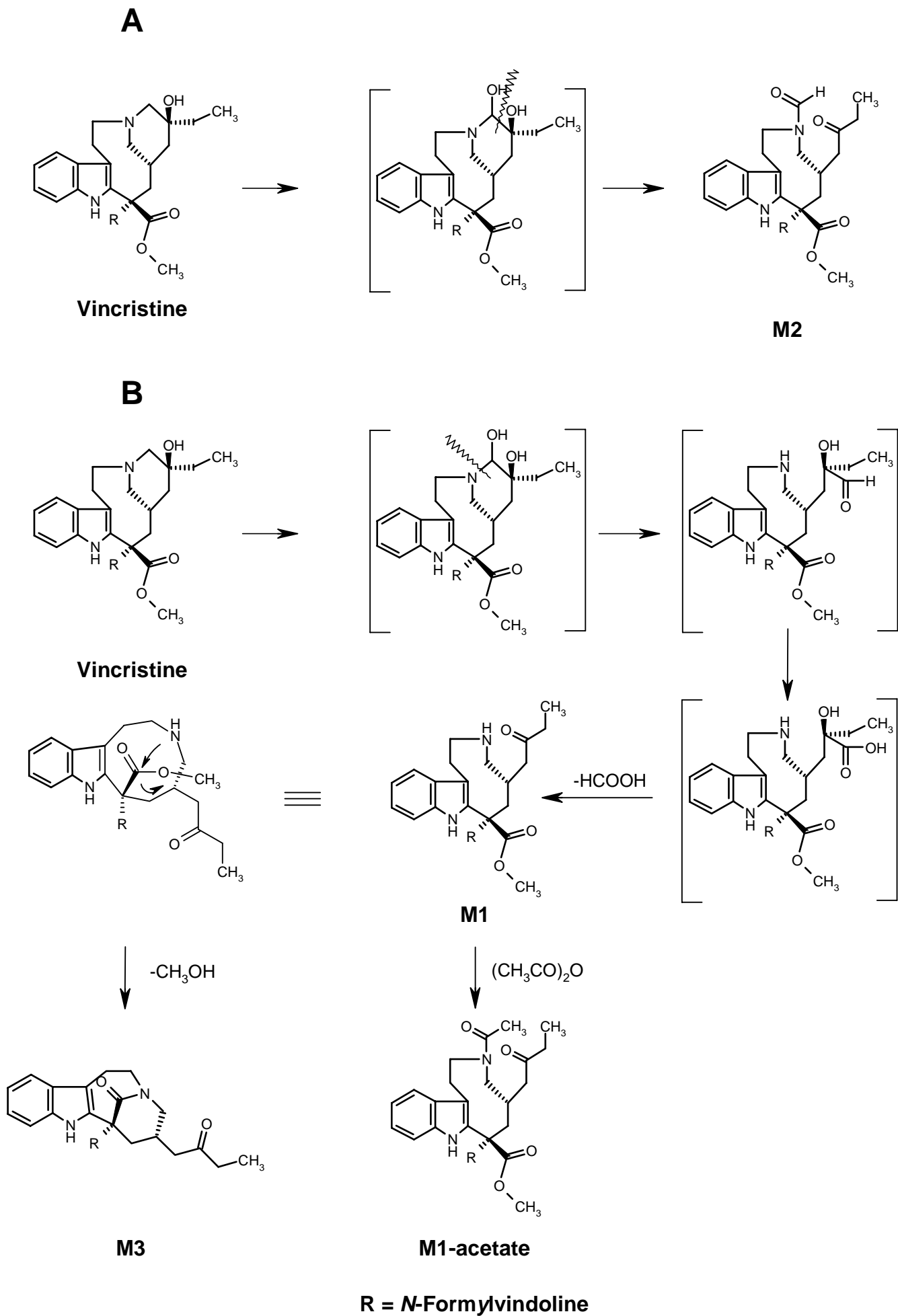


Fig. 6

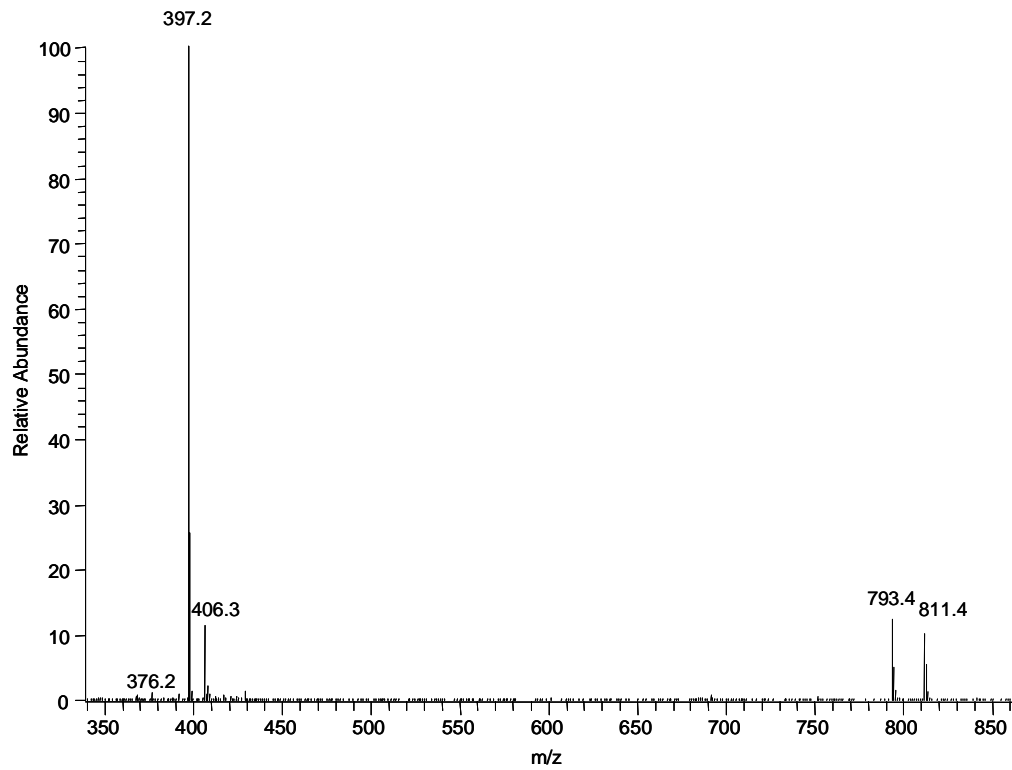


Fig. 7

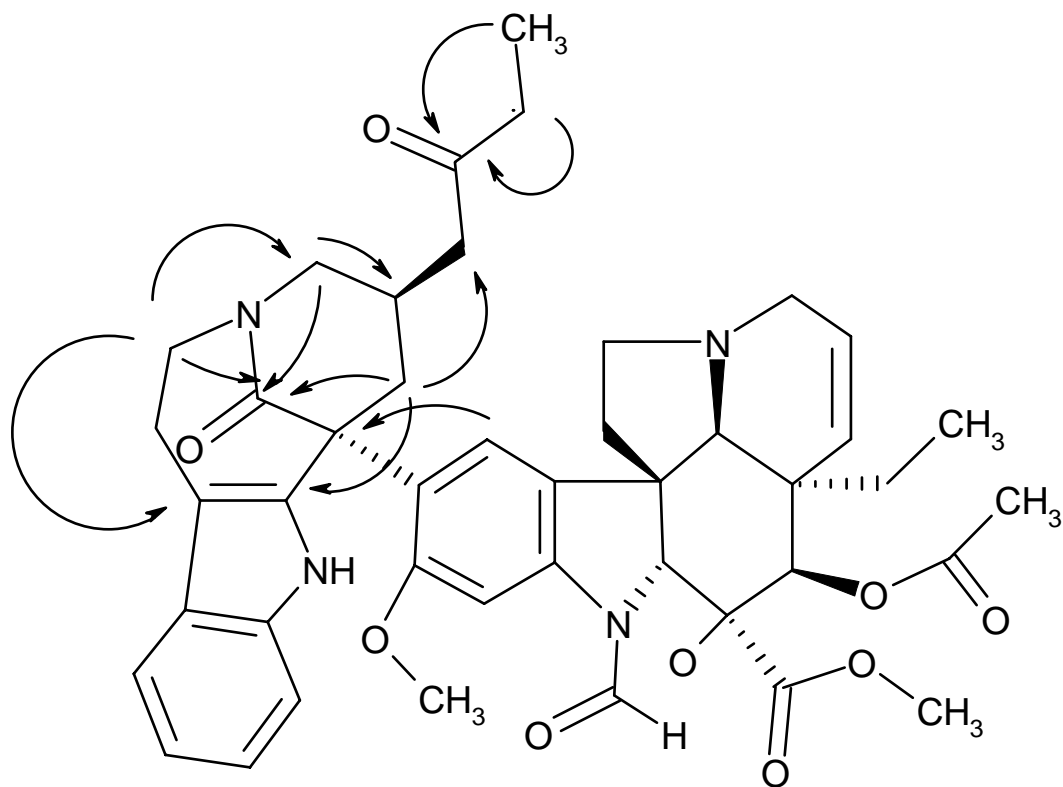


Fig. 8

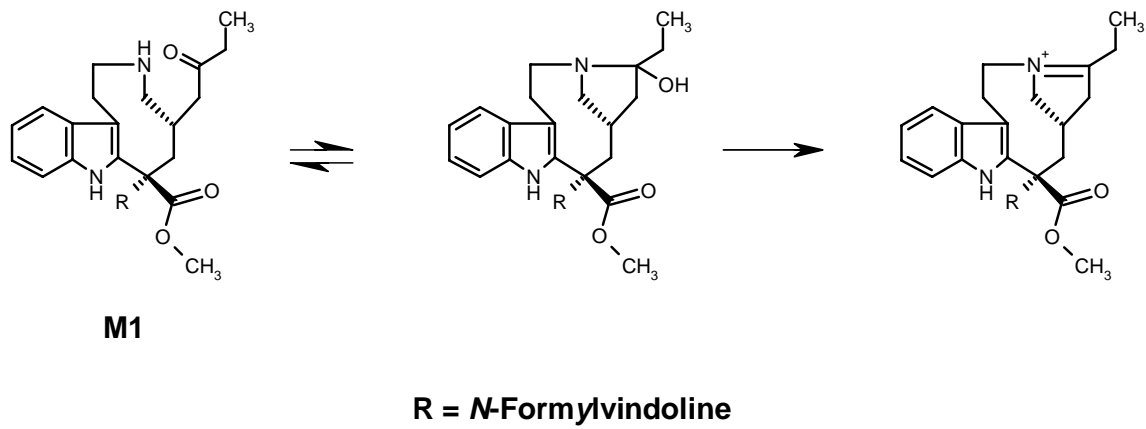


Fig. 9

